Measurement 167 (2021) 108256

Contents lists available at ScienceDirect

Measurement

journal homepage: www.elsevier.com/locate/measurement

# Concentration measurement without calibration of natural sediment particles using backscatter sensing with optical fibres

Rui Huang, Qinghe Zhang *

*State Key Laboratory of Hydraulic Engineering Simulation and Safety, Tianjin University, Tianjin 300072, China*

ARTICLE INFO

*Article history:*
Received 10 March 2020
Received in revised form 9 July 2020
Accepted 14 July 2020
Available online 24 July 2020

*Keywords:*
Optical backscatter
Optical fibre
Natural sediment
Sediment concentration
Characteristic particle size
Non-calibration measurement

ABSTRACT

A set of newly developed miniature optical fibre sediment concentration measuring instrument is used for the concentration measurement of natural sediments. Through calibration with natural sediments of different particle size distributions collected from different beaches in China, we establish two unified relations between natural sediment concentration and output voltage of optical backscatter intensity to obtain the natural sediment concentration without calibration. The concept of the compositional weighted sediment size is proposed to characterize the optical backscatter property of natural sediments, which is more accurate for non-calibration sediment concentration measurement. On the premise that particle size distribution of natural sediments is known, it is no longer necessary to calibrate sediment concentration, and the unified relations can be used to directly measure sediment concentration, which provides a new highly convenient concentration measurement method of natural sediments.



## 1. Introduction

Many morphological and ecological processes are associated with the transport of suspended sediments in estuarine and coastal waters [1–4]. The suspended sediment concentration has a great influence on the surrounding hydrodynamics and water environment [5,6]. Therefore, measuring the suspended sediment concentration has always been an important subject in laboratory and field investigations [7,8].

In recent years, various sediment concentration measurement methods, such as electrical method [9], acoustic method [10–12], optical method [13–15] and imaging method [16–18], have attained great progress [19–22]. Especially in regard to the measurement of the sediment concentration by the optical method [23], many commercial turbidimeters based on the principles of optical diffraction, backscatter and transmission have become standard products, such as the Sequoia Scientific Inc. LISST-100X, the Campbell Scientific Inc. OBS5+, the Hach 2100Q, etc. These commercial turbidimeters have been used for a large number of sediment concentration measurements in the laboratory and field [24–26].

At present, the probe sizes of most commercial turbidimeters are relatively large (~10 cm φ × 50 cm L). Although the influence of the probe size on the hydrodynamics in the field is relatively small, these probes are too large and cannot be regarded as nonintrusive in small laboratory flumes, such as when measuring the sediment concentration in an oscillating grid flume and settling column [27–29]. Most previous optical detection methods adopted an actuator-sensor mode to detect the scattered light of sediment particles [30], in which the actuator emits parallel incident beams through sediment suspensions, and the sensor receives directional scattered light from the sediment suspensions [31,32]. To miniaturize the sensing probe, researchers have used a single probe to measure the sediment concentration through synchronous light emission and reception based on the principle of optical transmission [33,34]. Recently, on the basis of the backscatter principle, Huang et al. designed a miniaturized measuring probe using optical fibres [35]. The diameter of the optical fibre probe immersed in water was only 2.5 mm, and the transmitting and receiving optical fibres were fixed together to form a 180° backscatter angle. The final multi-channel single-probe sediment concentration measuring instrument was able to measure the sediment concentration in a nearly non-intrusive manner.

Influenced by different factors, such as the particle size, colour and shape, the optical measurement method needs to be calibrated with each sediment sample to accurately obtain the sediment concentration. Considering that the particle size has the largest effect on the optical scattering characteristics of sediment particles and the effects of other factors are an order of magnitude smaller than that of the particle size [36–40], Huang et al. used a miniature fibre

* Corresponding author.
*E-mail address:* qhzhang@tju.edu.cn (Q. Zhang).

https://doi.org/10.1016/j.measurement.2020.108256
0263-2241/

optic concentration probe to develop a unified relationship for uniform silicon carbide particles [41]. With the silicon carbide particle size as the input parameter, the silicon carbide particle concentration for different particle sizes within the range of 38–250 μm was measured directly by using the unified relation, without the need for calibration. However, this relation is only suitable for uniform particles. A unified relation for non-uniform natural sediments remains to be established. Therefore, the objective of the present paper is to collect non-uniform natural sediments from different beaches and investigate the possibility of obtaining a unified relation of natural sediments with the newly developed miniature optical fibre concentration measurement instrument. Then we developed a method to measure the natural sediment concentration without calibration when the particle size distribution is known.

The outline of this paper is as follows. The measuring principle of the miniature optical fibre probe and the components of the multi-channel sediment concentration measurement instrument are introduced in Section 2. We analyse the particle size characteristics of nine natural sediment samples collected from coastal beaches in China and calibrate the relationship between the sediment concentration and voltage output of the optical backscatter intensity for six natural sediments in Section 3. Characteristic grain sizes are proposed and used as input parameters, and we establish and verify unified relations between the sediment concentration and optical backscatter intensity in Section 4. Conclusions are drawn in Section 5.

## 2. Measuring instrument

The sediment concentration measurement in this paper is based on the optical backscatter principle. The sediment suspension near the end face of the optical sensor is illuminated by a light beam emitted by optical fibres. As shown in Fig. 1, a 180° backscatter angle is attained by combining the optical fibre receiving scattered light with the optical fibres emitting light. In this way, the incidence of the emitted light and reception of the scattered light are integrated into a single probe, and the size of probe is reduced [42,43]. Among the components, the receiving fibre in the probe adopts a 1.5 mm plastic fibre in the centre of the probe. A set of 22 0.25 mm thin plastic fibres are arranged encircling the receiving fibre to transmit light generated by the light source. The structure of the fibre probe is shown in panel A of Fig. 1. The other end of the receiving optical fibre is connected to the photodetector DET36A(/M) (Thorlabs Inc., Newton, New Jersey, United States) to sense the change in backscatter light intensity, which is a biased, Silicon (Si) detector designed for detection of light signals ranging from 350 to 1100 nm. Its output voltage is 0–10 V. The performance parameters of the photodetector DET36A(/M) are listed in Table 1 [44]. The photodetector is connected to the data acquisition card, through which the analogue signal is converted into a digital signal to record the voltage level corresponding to the backscattered light in real time. The sketch of sediment concentration measuring principle is shown in Fig. 2. The calibrated relationship between the voltage signal and sediment concentration can be used to obtain the sediment concentration. The light source is an LED white visible cold light source, which is not easily absorbed by water and suitable for use in plastic fibres. Moreover, the white visible light source is inexpensive, easy to use, and the intensity of the light source can be adjusted, as shown by the red arrow in the instrument container of Fig. 1.

To easily use the instrument, the visible light source, photodetectors and data acquisition card are connected within a box, which can be used to control the operation and intensity of the light source on the panel. The photo of five-channel miniature

**Table 1**
The performance parameters of the photodetector DET36A(/M) [44].

| Performance parameters | Specifications |
|---|---|
| Detector | Silicon PIN |
| Active Area | 3.6 × 3.6 mm (13 $mm^2$) |
| Wavelength Range | 350–1100 nm |
| Peak Wavelength | 970 nm |
| Bias Voltage | 10 V |
| Output Voltage | 0–10 V |

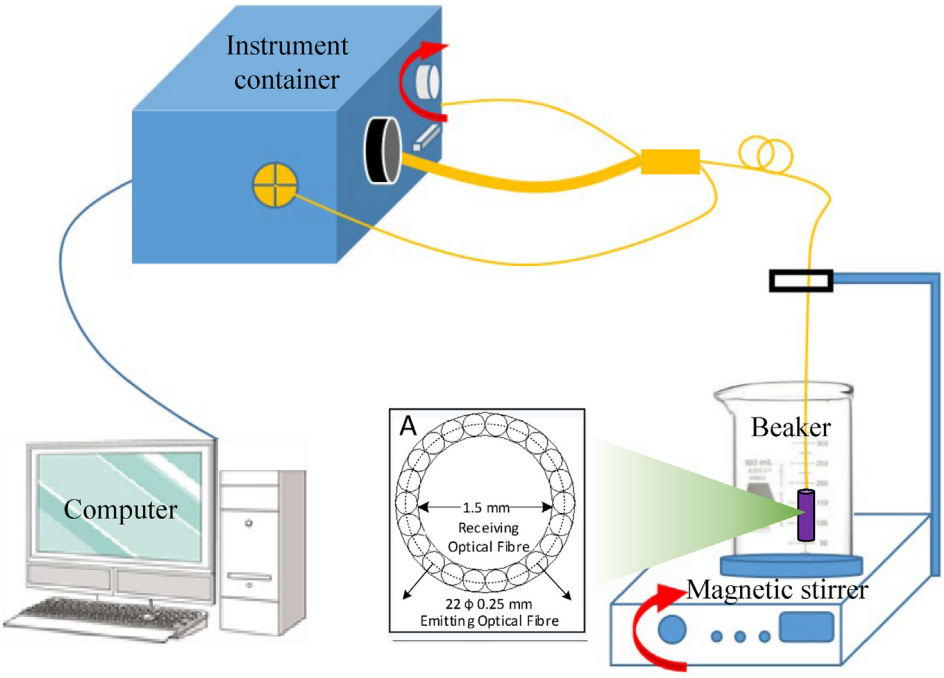


**Fig. 1.** Schematic diagram of the measurement equipment setup.

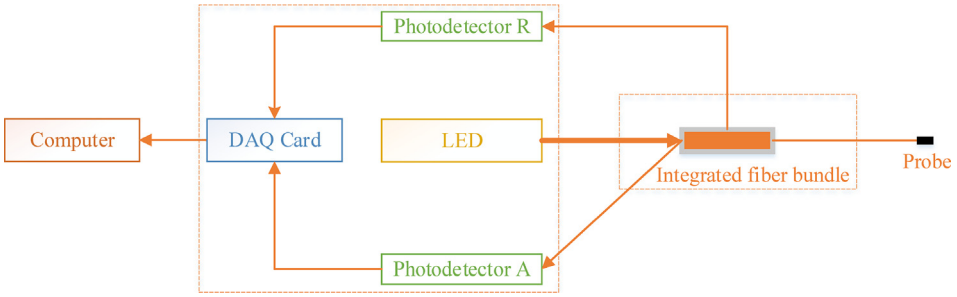


**Fig. 2.** Sketch of sediment concentration measuring principle.

**Fig. 3.** Five-channel miniature optical fibre sediment concentration measuring instrument.

optical fibre sediment concentration measuring instrument designed and manufactured based on optical backscatter is shown in Fig. 3. In practice, the sediment concentration can be directly measured by immersing the probe in the sediment suspension. The optical fibre probe is made of plastic fibres and protected by a metal case. The total diameter of the front end of the optical fibre probe is only 2.5 mm, which greatly reduces the disturbance of the probe to the surrounding water. In addition, plastic fibre has the advantages of light weight and damage resistance, which meet the requirements of daily convenient and stable use [45].

## 3. Concentration relationship calibration for natural sediments

### 3.1. Natural sediment collection and particle size analysis

We collected nine natural sediment samples from coastal beaches along the Bohai Sea, Zhejiang Province, Fujian Province and Hainan Province in China. The natural sediments were pre-processed by filtering to remove impurities and drying. Pictures of the nine natural sediment samples are shown in Fig. 4. A Malvern grain size analyser, the Mastersizer 3000 (Malvern Panalytical Ltd., Malvern, United Kingdom) was used to analyse the grain size of the natural sediments. The Mastersizer 3000 uses the technique of laser diffraction to measure the particle size and particle size distribution of materials, which delivers measurements from 10 nm to 3.5 mm using a single optical measurement path, making it suitable for an extremely wide range of applications. The performance parameters of the Mastersizer 3000 are listed in Table 2 [46]. The grading curves are shown in Fig. 5. $D_{10}$, $D_{50}$, and $D_{90}$ of the nine natural sediments are listed in Table 3. Among them, $D_{10}$, $D_{50}$ and $D_{90}$ represent the 10%, 50% and 90% fractions, respectively, of the total sediment weight that are smaller than this particle size. The median grain sizes of the nine natural sediment samples are generally distributed between 0.05 and 0.5 mm, and the grain size grading is relatively continuous. We use sediment samples A1, A2, A3, A4, A7 and A9 for concentration calibration, and sediment samples A5, 6 and 8 are used for verification.

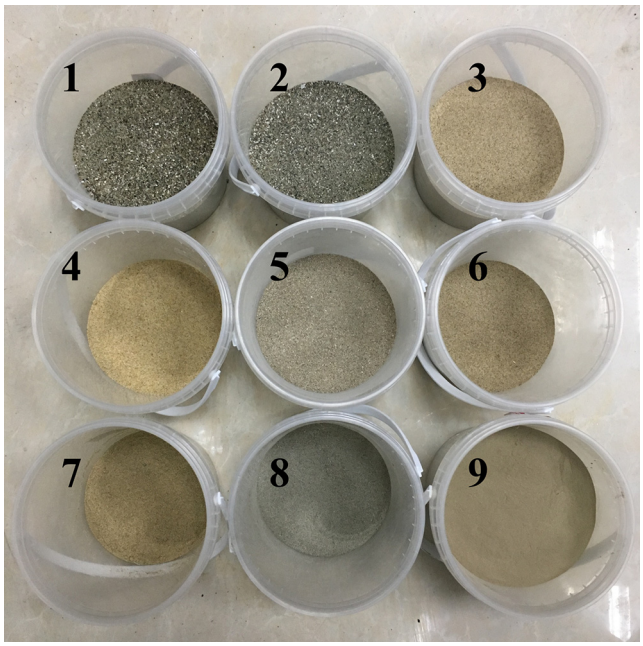


**Fig. 4.** Nine natural sediment samples.

**Table 2**
The performance parameters of the Mastersizer 3000 [46].

| Performance parameters | Specifications |
|---|---|
| Materials | Suspensions, emulsions, dry powders |
| Principle | Laser light scattering |
| Analysis | Mie and Fraunhofer scattering |
| Data acquisition rate | 10 kHz |
| Typical measurement time | <10 sec |
| Size range | 10 nm–3.5 mm |
| Accuracy | Better than 0.6% |

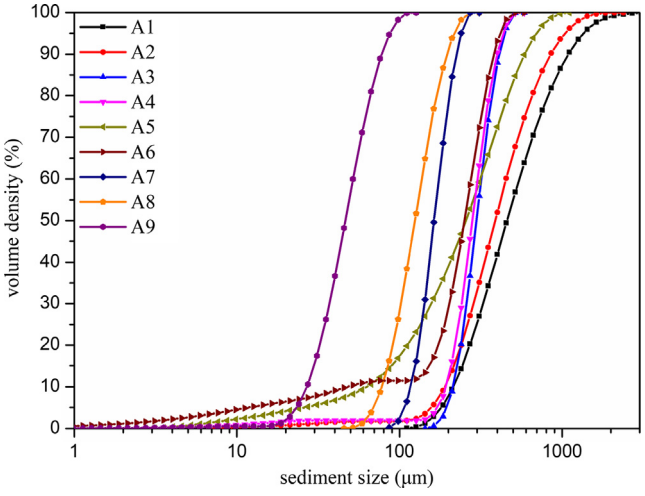


**Fig. 5.** Grain size grading curves of the nine natural sediment samples.

**Table 3**
Particle size distribution of the nine natural sediments.

| Sample number | $D_{10}$ (μm) | $D_{50}$ (μm) | $D_{90}$ (μm) | $D_w$ (μm) |
|---|---|---|---|---|
| A1 | 215 | 458 | 1090 | 612.75 |
| A2 | 190 | 388 | 854 | 494.18 |
| A3 | 214 | 298 | 412 | 325.85 |
| A4 | 192 | 281 | 398 | 269.16 |
| A5 | 63 | 257 | 589 | 315.43 |
| A6 | 51 | 252 | 380 | 230.17 |
| A7 | 117 | 164 | 225 | 157.17 |
| A8 | 78 | 125 | 197 | 123.34 |
| A9 | 27 | 47 | 78 | 52.91 |

### 3.2. Concentration relationship calibration

Uniform suspensions with different standard sediment concentrations are prepared in beaker with magnetic stirrer to calibrate the concentration [47]. The rotation speed of the magnetic stirrer can be adjusted so that more uniform sediment suspension can be obtained, as shown by the red arrow in the magnetic stirrer of Fig. 1. After adjusting the intensity of the LED light source, sediment samples A1, A2, A3, A4, A7 and A9 were used to calibrate the relationship between the concentration and output voltage. The calibration curves are shown in Fig. 6.

It can be clearly seen that the concentrations of the six natural sediment samples have a linear relation with the voltage at low concentrations, and the change in concentration has a great influence on the backscatter intensity. However, at high concentrations, the relationship between the concentration and backscatter intensity is nonlinear, and the backscatter intensity varies very slightly

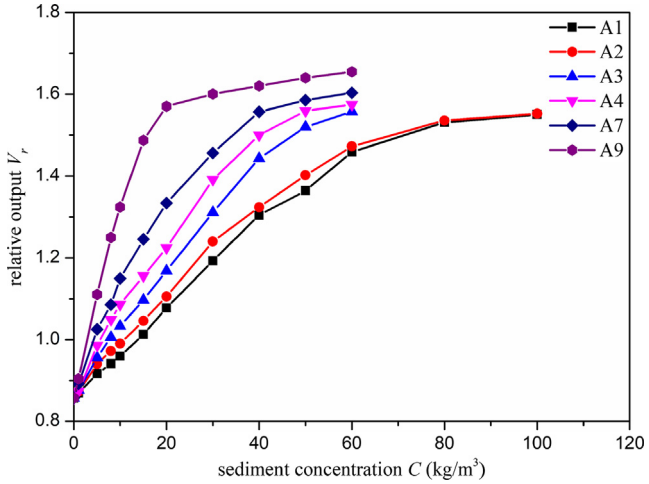


**Fig. 6.** Concentration-voltage relationship curves of the six natural sediments.

with the concentration. This mainly occurs because the number of sediment particles is small when the sediment concentration is low, and the degree to which the incident light is backscattered by sediment particles is mainly proportional to the number of sediment particles. When the sediment concentration is high, more sediment particles will lead to a slow increase in backscatter light intensity due to the multiple particles backscattering light, which results in the relationship between the sediment concentration and output voltage in the high-concentration section no longer being linear but nearly curvilinear [48].

In addition, it can be observed that the voltages of sediment samples A1 and A2 have clear positive correlations with the concentration in the range of 0–100 kg/m$^3$, while the voltages of sediment samples A3, A4, A7 and A9 have positive correlations with the concentration in the range of 0–60 kg/m$^3$. The different measuring ranges for the sediments with different sizes can be explained as follows. For particles with different sizes at the same sediment concentration, the smaller the particle size is, the more particles there are in the suspension, and the higher the backscatter light intensity generated by the particles will be. Therefore, small-sized sediment particles tend to reach backscattered light saturation at low concentrations and show a small detectable concentration range. Considering that the linear correlation between the sediment concentration and output voltage can significantly improve the measurement accuracy, we analysed the approximate linear range at low concentrations for the six natural sediments. The approximately linear distribution ranges of sediment samples A1, A2, A3, A4, A7 and A9 are 0–40, 0–30, 0–30, 0–20, 0–15 and 0–10 kg/m$^3$, respectively. The linear range increases with increasing particle size.

Linear fitting is carried out for the linear concentration-voltage sections of the six sediment samples, and the calibration relations are shown in Fig. 7.

Linear function Eq. (1) is adopted for data fitting, where $a$ and $V_w$ are fitting coefficients, $C$ is the sediment concentration (kg/m$^3$), and $V_r$ is the relative value of the voltage $V_A$ corresponding to the backscatter light intensity that eliminates the voltage fluctuation $V_R$ of the light source in Eq. (2):

$$V_r = a \times C + V_w \tag{1}$$

$$V_r = \frac{V_A}{V_R} \tag{2}$$

When $C$ is 0, that is, the backscatter light intensity of the pure water background is consistent. Since the diameter of the receiving optical fibre in the optical fibre probe is only 1.5 mm and the

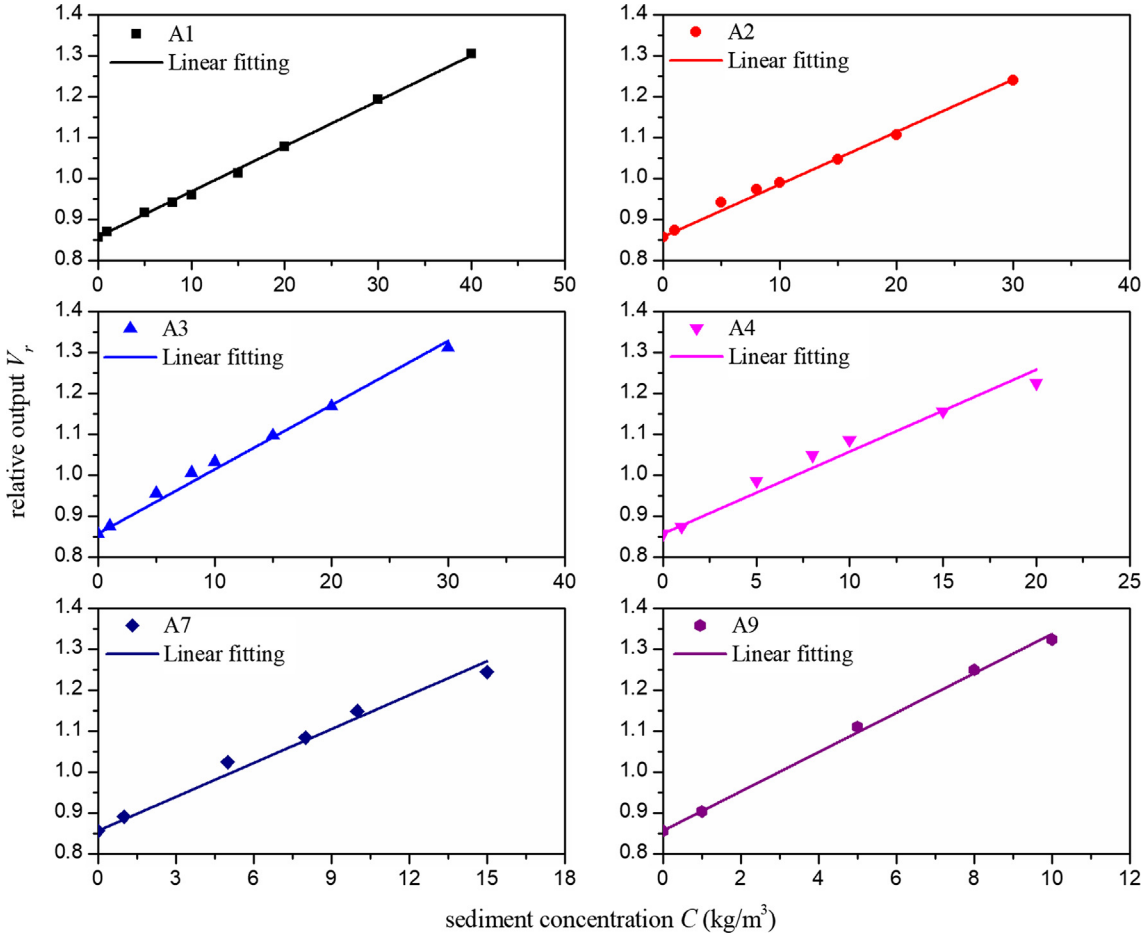


**Fig. 7.** Linear fitting of the concentration-voltage relationships of the six natural sediments.

**Table 4**
Parameters of linear fitting for the six natural sediments.

| Sample number | $a$ | $R^2$ | Regression error |
|---|---|---|---|
| A1 | 0.0111 | 0.9999 | 9.8365E−5 |
| A2 | 0.0128 | 0.9999 | 2.3203E−4 |
| A3 | 0.0157 | 0.9998 | 3.6622E−4 |
| A4 | 0.0200 | 0.9994 | 8.7230E−4 |
| A7 | 0.0276 | 0.9997 | 9.6723E−4 |
| A9 | 0.0481 | 0.9999 | 7.5554E−4 |

optical fibre probe basically only receives an optical signal near the end face of the probe, the change in background light has no effect on $V_w$ [49]. We obtained the value of $V_w$ as:

$$V_w = 0.857 \tag{3}$$

The fitting parameters of the six natural sediments are summarized in Table 4. The fitting correlation coefficients $R^2$ of the six natural sediments are higher than 0.99 and regression errors are all less than 1E−3. The linear fitting degree is high.

## 4. Unified relations for non-calibration measurement of natural sediments

To measure the sediment concentration using the optical backscatter method, the particle size has the greatest influence on the backscattered light [50–53]. From the concentration-voltage relations of the six natural sediment samples in Section 3.2, it can be seen that the backscatter light intensity of the sediment particles increases with decreasing particle size at the same concentration, which shows that the slope $a$ of the linear fitting function is larger. In the following section, we attempt to find the characteristic grain size of the natural sediments to establish a unified relation between coefficient $a$ and the characteristic grain size.

### 4.1. Characteristic grain size of natural sediments

#### 4.1.1. The median size

The median particle size $D_{50}$ of natural sediments represents the particle size that accounts for 50% of the total weight of the particles in natural sediment grading, and it is widely used in sediment transport research. We tried to establish a relation between natural sediment grading and optical backscatter intensity by using the median particle size $D_{50}$. The relationship between the median particle size $D_{50}$ of the six natural sediments and slope $a_m$ of the linear fitting equation is shown in Fig. 8.

The approximate relationship between the median particle size $D_{50}$ and slope $a_m$ is approximated by the reciprocal function. The correlation coefficient $R^2$ = 0.989 of fitting equation indicates a high degree of correlation.

$$a_m = 11.330/(D_{50} + 156.205) - 0.008 \tag{4}$$

#### 4.1.2. The compositional weighted size

To characterize the comprehensive backscatter effect of natural sediments reasonably and accurately, we must reflect the backscatter effect of all particle sizes in natural sediments.

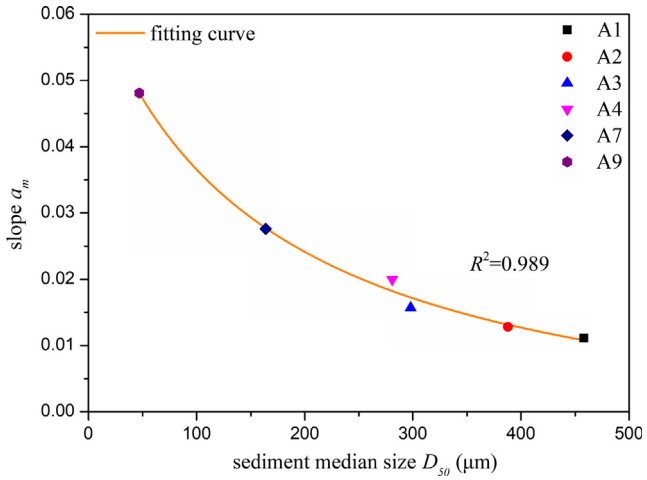


**Fig. 8.** Fitting curve for median size $D_{50}$ and slope $a_m$ of the natural sediments.

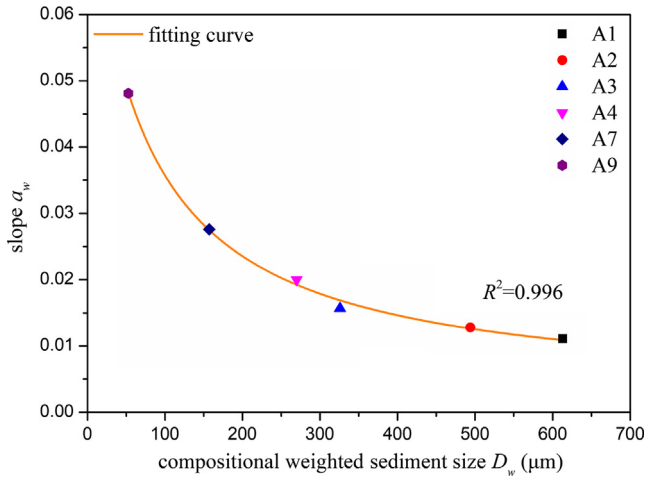


**Fig. 9.** Fitting curve for compositional weighted size $D_w$ and slope $a_w$ of the natural sediments.

Therefore, the comprehensive optical backscatter effect of all particle sizes of natural sediments should be characterized by a characteristic particle size of the compositional weight of the sediment particle size. The compositional weighted particle size of natural sediments is expressed as:

$$D_w = \sum_n \varphi_n D_n \tag{5}$$

where $D_w$ represents the characteristic particle size calculated according to the weight of each particle size in natural sediments, $\varphi_n$ is the percentage of component $n$ in natural sediments, and $D_n$ is the particle size of component $n$ in natural sediments. The exact calculation formula of compositional weighted particle size is:

$$D_w = \int_{D_{\min}}^{D_{\max}} D \cdot \varphi(D) dD \tag{6}$$

where $\varphi(D)$ is the volumetric percentage function measured by the Malvern particle size analyser with the change in particle size, and $D_{min}$ and $D_{max}$ are the minimum and maximum particle sizes of the natural sediment grading, respectively. For convenience, the compositional weighted characteristic particle sizes of the nine natural sediments calculated from the grading curve of Fig. 5 are also listed in Table 3.

The compositional weighted particle size of natural sediments is the weighted particle size representing the proportion of each particle size in natural sediment grading. The relationship between the weighted particle size $D_w$ of the six natural sediments and slope $a_w$ of the linear fitting equation is shown in Fig. 9.

The approximate relationship between the compositional weighted particle size $D_w$ and slope $a_w$ is approximated by the reciprocal function of Eq. (7). The correlation coefficient $R^2$ = 0.996 indicates a high degree of correlation.

$$a_w = 5.764/(D_w + 73.345) + 0.002 \tag{7}$$

It can be seen from Figs. 8 and 9 that the fitting degree between the compositional weighted particle size and slope $a_w$ is higher than that between the median particle size and slope $a_m$. In addition, slope $a_m$ and $a_w$ shows a higher dependence on the median size and compositional weighted particle size smaller than 100 μm. This means that a small change in particle size within the range below 100 μm would lead to a large change in slope $a_m$ and $a_w$, while a change in particle size above 100 μm would have a small effect on slope $a_m$ and $a_w$, which is consistent with previous conclusions [54,55]. We use sediment concentration 20 kg/m$^3$ of sample A3 as an example. The error is 3.2% and 7.9% respectively using unified relation (8) of the median particle size $D_{50}$ when ignoring the particle size larger than 400 μm and 350 μm. The error is 0.5% and 4.5% respectively using unified relation (9) of the compositional weighted particle size $D_w$ when ignoring the particle size larger than 500 μm and 400 μm. It can be seen that ignoring the larger particle size has little influence on the accuracy of concentration measurement. This phenomenon has great implications for the measurement of the natural sediment concentration by the optical backscatter method. When $D_{50}$ is larger than 400 μm, as shown in Fig. 8, and $D_w$ is larger than 500 μm, as shown in Fig. 9, the change in sediment particle size has little effect on slope $a_m$ and $a_w$. When the measurement accuracy does not have to be high, the effect of the particle size can be ignored for coarse particles larger than 500 μm.

### 4.2. Unified concentration measurement relations of natural sediments

The fitting relationship of the median size (Eq. (4)), the fitting relationship of the compositional weighted size (Eq. (7)), and the relationship of the sediment concentration and voltage (Eqs. (1) and (3)) form the following unified relations, Eqs. (8) and (9):

$$V_{rm} = (11.330/(D_{50} + 156.205) - 0.008)C + 0.857 \tag{8}$$

$$V_{rw} = (5.764/(D_w + 73.345) + 0.002)C + 0.857 \tag{9}$$

The applicable range of the unified relations in Eqs. (8) and (9) is the linear range of the relation between the natural sediment concentration and voltage with different characteristic particle sizes. By fitting the concentration measurement range corresponding to the different characteristic particle sizes of the natural sediments in Fig. 7, the fitting concentration measurement ranges corresponding to the median sediment size and compositional weighted sediment size are shown in Fig. 10. The corresponding fitting equations are Eqs. (10) and (11), respectively:

$$C_m = 3.859 \times \exp(D_{50}/209.889) + 5.662 \tag{10}$$

$$C_w = 21.858 \times \exp(D_w/702.586) - 12.890 \tag{11}$$

### 4.3. Verification of the non-calibration concentration measurement of natural sediments

Natural sediment samples A5, A6 and A8 are used to verify the accuracy of the unified relations. The non-calibration

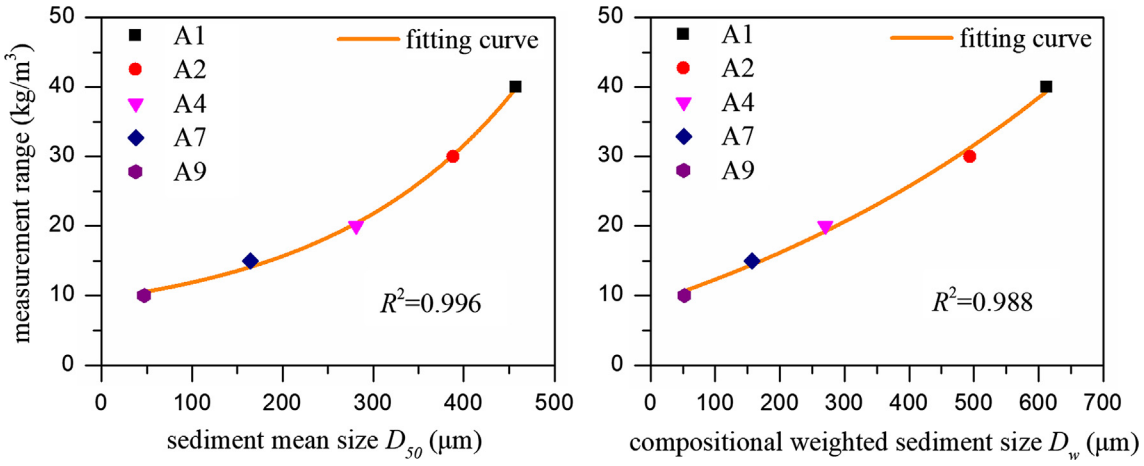


**Fig. 10.** The concentration measurement range of natural sediment with different characteristic particle sizes.

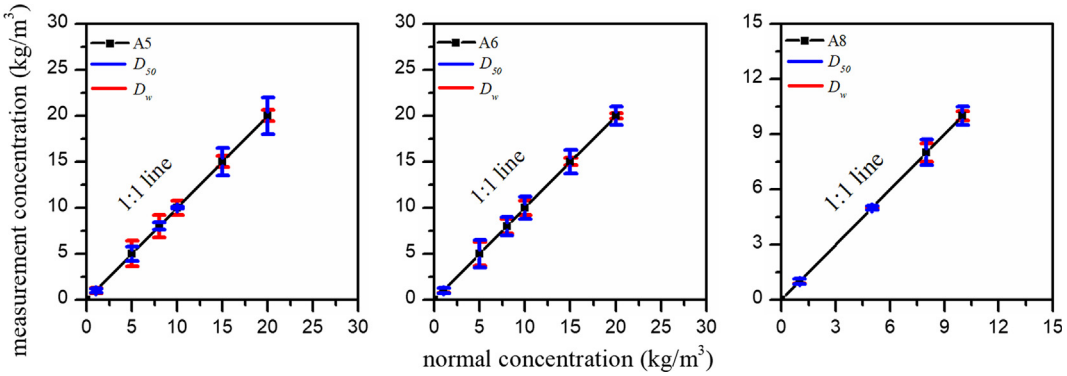


**Fig. 11.** Non-calibration concentration measurement errors of the three natural sediments.

concentration measurement errors of sediment samples A5, A6 and A8 using Eqs. (8) and (9) are shown in Fig. 11. The relative errors at high concentrations above 5 kg/m$^3$ for the three natural sediment samples using the two unified relations are mostly within 10%. However, the measurement errors in the low-concentration range, below 5 kg/m$^3$, is slightly larger, and the relative errors are within 30%. This mainly occurs because the number of sediment particles in the low-concentration range is smaller, the backscatter light intensity of the sediment particles is low, and the measurement accuracy is relatively low. The results of Fig. 11 indicate that using the median particle size and compositional weighted particle size of natural sediments as input parameters, the unified calibrated relations in this paper can be used to directly obtain the concentration of natural sediments, and no calibration is required. This method greatly improves the convenience of measuring the natural sediment concentration.

**Table 5**
Comparison of the non-calibration measurement errors of three kinds of natural sediments (kg/m$^3$).

| *Verification Concentration* | A5 | | A6 | | A8 | |
|---|---|---|---|---|---|---|
| | $D_{50}$ | $D_w$ | $D_{50}$ | $D_w$ | $D_{50}$ | $D_w$ |
| 1.0 | 0.2 | 0.3 | 0.3 | 0.25 | 0.15 | 0.12 |
| 5.0 | 0.8 | 1.4 | 1.5 | 1.3 | 0.1 | 0.06 |
| 8.0 | 0.4 | 1.2 | 1.0 | 0.8 | 0.7 | 0.5 |
| 10.0 | 0.1 | 0.8 | 1.2 | 0.8 | 0.5 | 0.25 |
| 15.0 | 1.5 | 0.6 | 1.3 | 0.4 | \ | \ |
| 20.0 | 2.0 | 0.6 | 1.0 | 0.3 | \ | \ |

In addition, a comparison of the non-calibration measurement errors of the three natural sediments is provided in Table 5. It can be seen from the non-calibration measurement results of sediment samples A5, A6 and A8 in Table 3, apart from the low-concentration range of sediment sample A5, the unified relation of the compositional weighted size has a higher accuracy than that of the median particle size. This occurs mainly because the compositional weighted particle size of sediments represents the comprehensive effect of all particle sizes. Therefore, in the non-calibration concentration measurements of sediments A5, A6 and A8, the results of the compositional weighted particle size are superior to the results of the median particle size. However, for the low-concentration range of sediment A5, because the particle size of sediment A5 is relatively larger, the number of particles is much smaller, the backscatter light is lower, and the measurement precision is relatively low. The unified relation of the median particle size is slightly better than that of the compositional weighted size at low concentrations of relatively coarse sediments.

The non-calibration measurement of the compositional weighted size is significantly better than that of the median size for natural sediments consisting of fine particles, and the unified relation of the compositional weighted size improves the non-calibration measurement precision.

## 5. Conclusions

The recently developed miniature optical fibre sediment concentration measuring instrument based on the optical backscatter method is used to establish a non-calibration method

for measuring the natural sediment concentration. Six natural sediment samples collected from coastal beaches in China are used for concentration calibration. To improve the measurement accuracy, we analysed the approximate linear range at low concentrations for the six natural sediments. The high fitting correlation coefficients $R^2$ and minor regression errors indicate that the linear fitting degree is high. Adopting the characteristic particle size based on the median particle size $D_{50}$ and compositional weighted particle size $D_w$ as input parameter, two unified relations between the concentration and optical backscatter intensity are established. Based on the unified relations, the concentration of any natural sediment can be directly obtained without calibration on the premise that the natural sediment particle size distribution is known. This method is a highly convenient and accurate practical measurement approach.

The non-calibration sediment concentration measurement method is suitable for known median particle size $D_{50}$ and compositional weighted particle size $D_w$ of the measured sediment. The method is particularly applicable for sediment concentration measurement in the laboratory, in which situation we can measure the sediment size distribution in advance. In practical applications, the suspended sediment particle size distribution is often measured through hydrologic observation during tidal cycles at fixed stations in field [56,57]. Therefore, the two unified relations based on the the median particle size $D_{50}$ and compositional weighted particle size $D_w$ are also appropriate in practical applications. In order to further improve the measurement convenience and accuracy, the synchronous measurement of sediment particle size distribution and sediment concentration is the aim of our future research.

## CRediT authorship contribution statement

**Rui Huang:** Conceptualization, Data curation, Methodology, Formal analysis, Writing - original draft. **Qinghe Zhang:** Conceptualization, Data curation, Methodology, Formal analysis, Writing - review & editing, Funding acquisition.

## Declaration of Competing Interest

The authors declare that they have no known competing financial interests or personal relationships that could have appeared to influence the work reported in this paper.

## Acknowledgements

This research is funded by the National Natural Science Foundation of China (No. 51679161). The authors sincerely thank the editor and anonymous reviewers for improving the manuscript.

## References

[1] L.C. Van Rijn, Principles of Sediment Transport in Rivers, Estuaries and Coastal Seas, Aqua Publications, Amsterdam, 1993.
[2] N. Haregeweyn, J. Poesen, J. Nyssen, J. De Wit, M. Haile, G. Govers, S. Deckers, Reservoirs in Tigray (Northern Ethiopia): Characteristics and sediment deposition problems, Land Degrad. Dev. 17 (2006) 211–230, https://doi.org/10.1002/ldr.698.
[3] D.J. Jerolmack, C. Paola, Shredding of environmental signals by sediment transport, Geophys. Res. Lett. 37 (2010) L19401, https://doi.org/10.1029/2010GL044638.
[4] K. Vercruysse, R.C. Grabowski, R.J. Rickson, Suspended sediment transport dynamics in rivers: Multi-scale drivers of temporal variation, Earth-Sci. Rev. 166 (2017) 38–52, https://doi.org/10.1016/j.earscirev.2016.12.016.
[5] A.J. Mehta, E.J. Hayter, W.R. Parker, R.B. Krone, A.M. Teeter, Cohesive sediment transport. I: Process description, J. Hydraul. Eng.-ASCE 115 (1989) 1076–1093, https://doi.org/10.1061/(asce)0733-9429(1989)115:8(1076).
[6] A. Mhashhash, B. Bockelmann-Evans, S.Q. Pan, Effect of hydrodynamics factors on sediment flocculation processes in estuaries, J. Soils Sediments 18 (2018) 3094–3103, https://doi.org/10.1007/s11368-017-1837-7.
[7] V.I. Nikora, D.G. Goring, Fluctuations of suspended sediment concentration and turbulent sediment fluxes in an open-channel flow, J. Hydraul. Eng.-ASCE 128 (2002) 214–224, https://doi.org/10.1061/(ASCE)0733-9429(2002)128:2(214).
[8] G. Voulgaris, S.T. Meyers, Temporal variability of hydrodynamics, sediment concentration and sediment settling velocity in a tidal creek, Cont. Shelf Res. 24 (2004) 1659–1683, https://doi.org/10.1016/j.csr.2004.05.006.
[9] P.N. Mishra, T. Bore, Y. Jiang, A. Scheuermann, L. Li, Dielectric spectroscopy measurements on kaolin suspensions for sediment concentration monitoring, Measurement 121 (2018) 160–169, https://doi.org/10.1016/j.measurement.2018.02.034.
[10] J.W. Gartner, Estimating suspended solids concentrations from backscatter intensity measured by acoustic Doppler current profiler in San Francisco Bay, California, Mar. Geol. 211 (2004) 169–187, https://doi.org/10.1016/j.margeo.2004.07.001.
[11] P.D. Thorne, D. Hurther, An overview on the use of backscattered sound for measuring suspended particle size and concentration profiles in non-cohesive inorganic sediment transport studies, Cont. Shelf Res. 73 (2014) 97–118, https://doi.org/10.1016/j.csr.2013.10.017.
[12] B.C. Xaiver, I.O. Silva, L.G. Guimaraes, M.N. Gallo, C.P. Ribeiro, A.G. Figueiredo, Estimation of suspended sediment concentration by acoustic scattering: an experimental and theoretical analysis for spherical particles, J. Soils Sediments 14 (2014) 1325–1333, https://doi.org/10.1007/s11368-014-0905-5.
[13] D. Pavanelli, A. Bigi, Indirect methods to estimate suspended sediment concentration: reliability and relationship of turbidity and settleable solids, Biosyst. Eng. 90 (2005) 75–83, https://doi.org/10.1016/j.biosystemseng. 2004.09.001.
[14] P.G. Minella Jean, G.H. Merten, J.M. Reichert, R.T. Clarke, Estimating suspended sediment concentrations from turbidity measurements and the calibration problem, Hydrol. Process. 22 (2008) 1819–1830, https://doi.org/10.1002/hyp.6763.
[15] J. Whinney, R. Jones, A. Duckworth, P. Ridd, Continuous in situ monitoring of sediment deposition in shallow benthic environments, Coral Reefs 36 (2017) 521–533, https://doi.org/10.1007/s00338-016-1536-7.
[16] X.J. Zou, H. Song, C.Y. Wang, Z.M. Ma, Relationships between B-mode ultrasound imaging signals and suspended sediment concentrations, Measurement 92 (2016) 34–41, https://doi.org/10.1016/j.measurement.2016.05.083.
[17] X.T. Shen, J.P.Y. Maa, A camera and image processing system for floc size distributions of suspended particles, Mar. Geol. 376 (2016) 132–146, https://doi.org/10.1016/j.margeo.2016.03.009.
[18] P.F. Qi, L. Lin, R. Huang, S.C. Zhao, H.L. Tian, S. Li, Q.H. Zhang, W.W. Liu, Image fiber-based miniature suspended solid sensor with high accuracy and a large dynamic range, Sci. Rep. 7 (2017) 16798, https://doi.org/10.1038/s41598-017-17003-y.
[19] J.R. Gray, J.W. Gartner, Technological advances in suspended-sediment surrogate monitoring, Water Resour. Res. 45 (2009) W00D29, https://doi.org/10.1029/2008WR007063.
[20] A.K. Rai, A. Kumar, Continuous measurement of suspended sediment concentration: Technological advancement and future outlook, Measurement 76 (2015) 209–227, https://doi.org/10.1016/j.measurement.2015.08.013.
[21] D. Felix, I. Albayrak, R.M. Boes, Continuous measurement of suspended sediment concentration: Discussion of four techniques, Measurement 89 (2016) 44–47, https://doi.org/10.1016/j.measurement.2016.03.066.
[22] D. Felix, I. Albayrak, R.M. Boes, In-situ investigation on real-time suspended sediment measurement techniques: Turbidimetry, acoustic attenuation, laser diffraction (LISST) and vibrating tube densimetry, Int. J. Sediment Res. 33 (2018) 3–17, https://doi.org/10.1016/j.ijsrc.2017.11.003.
[23] J. Downing, Twenty-five years with OBS sensors: The good, the bad, and the ugly, Cont. Shelf Res. 26 (2006) 2299–2318, https://doi.org/10.1016/j.csr.2006.07.018.
[24] J.P.Y. Maa, J.P. Xu, M. Victor, Notes on the performance of an optical backscatter sensor for cohesive sediments, Mar. Geol. 104 (1992) 215–218, https://doi.org/10.1016/0025-3227(92)90096-z.
[25] C.P. Holliday, T.C. Rasmussen, W.P. Miller, Establishing the Relationship Between Turbidity and Total Suspended Sediment Concentration, Georgia Institute of Technology, 2003.
[26] C.G. Campbell, D.T. Laycak, W. Hoppes, N.T. Tran, F.G. Shi, High concentration suspended sediment measurements using a continuous fiber optic in-stream transmissometer, J. Hydrol. 311 (2005) 244–253, https://doi.org/10.1016/j.jhydrol.2005.01.026.
[27] A.J.S. Cuthbertson, P. Dong, P.A. Davies, Non-equilibrium flocculation characteristics of fine-grained sediments in grid-generated turbulent flow, Coast. Eng. 57 (2010) 447–460, https://doi.org/10.1016/j.coastaleng.2009.11.011.
[28] M. Mory, N. Gratiot, A.J. Manning, H. Michallet, CBS layers in a diffusive turbulence grid oscillation experiment, Proc. Mar. Sci. 5 (2002) 139–154.
[29] V. Wendling, N. Gratiot, C. Legout, I.G. Droppo, C. Coulaud, B. Mercier, Using an optical settling column to assess suspension characteristics within the free, flocculation, and hindered settling regimes, J. Soils Sediments 15 (2015) 1991–2003, https://doi.org/10.1007/s11368-015-1135-1.
[30] L. Ma, F.J. Duan, G.C. Song, L. Zhao, A concentration measurement model of suspended solids in oilfield reinjection water based on underwater scattering, Measurement 117 (2018) 125–132, https://doi.org/10.1016/j.measurement.2017.11.061.
[31] L. Wind, W.W. Szymanski, Quantification of scattering corrections to the Beer-Lambert law for transmittance measurements in turbid media, Meas. Sci. Technol. 13 (2002) 270–275, https://doi.org/10.1088/0957-0233/13/3/306.

[32] A.F. Bin Omar, M.Z. Bin MatJafri, Turbidimeter design and analysis: a review on optical fiber sensors for the measurement of water turbidity, Sensors 9 (2009) 8311–8335, https://doi.org/10.3390/s91008311.
[33] H.Q. Wang, J.T. Hu, W. Wan, H.Q. Gui, F.H. Qin, F.J. Yu, J.G. Liu, L. Lu, A wide dynamic range and high resolution all-fiber-optic turbidity measurement system based on single photon detection technique, Measurement 134 (2019) 820–824, https://doi.org/10.1016/j.measurement.2018.12.012.
[34] R. Wang, G.L. Yu, Suspended sediment concentration measurement based on optical fiber technology, Meas. Sci. Technol. 30 (2019) 075205, https://doi.org/10.1088/1361-6501/ab188d.
[35] R. Huang, Q.H. Zhang, E.B. Xing, P.F. Qi, W.W. Liu, Multichannel measurement method of suspended sediment concentration based on optical fiber sensing, J. Hydroelectr. Eng. 38 (2019) 19–27.
[36] K.A. Ludwig, D.M. Hanes, A laboratory evaluation of optical backscatterance suspended solids sensors exposed to sand-mud mixtures, Mar. Geol. 94 (1990) 173–179, https://doi.org/10.1016/0025-3227(90)90111-v.
[37] C.S. Conner, A.M. De Visser, A laboratory investigation of particle size effects on an optical backscatterance sensor, Mar. Geol. 108 (1992) 151–159, https://doi.org/10.1016/0025-3227(92)90169-i.
[38] T.F. Sutherland, P.M. Lane, C.L. Amos, J. Downing, The calibration of optical backscatter sensors for suspended sediment of varying darkness levels, Mar. Geol. 162 (2000) 587–597, https://doi.org/10.1016/S0025-3227(99)00080-8.
[39] D.G. Bowers, C.E. Binding, The optical properties of mineral suspended particles: A review and synthesis, Estuar. Coast. Shelf Sci. 67 (2006) 219–230, https://doi.org/10.1016/j.ecss.2005.11.010.
[40] G.H. Merten, P.D. Capel, P.G. Minella, Effects of suspended sediment concentration and grain size on three optical turbidity sensors, J. Soils Sediments 14 (2014) 1235–1241, https://doi.org/10.1007/s11368-013-0813-0.
[41] R. Huang, Q.H. Zhang, P.F. Qi, W.W. Liu, Concentration measurement of uniform particles based on backscatter sensing of optical fibers, Water 11 (2019) 1955, https://doi.org/10.3390/w11091955.
[42] M.R. Shenoy, Optical fibre probes in the measurement of scattered light: Application for sensing turbidity, Pramana-J. Phys. 82 (2014) 39–48, https://doi.org/10.1007/s12043-013-0641-1.
[43] A.F. Omar, M.Z.M. Jafri, Optical System in Measurement of Water Turbidity: Design and Analytical Approach (Penerbit USM), Penerbit USM, 2015.
[44] https://www.thorlabschina.cn/drawings/53ce578195bd3c2b-280A16D1-FF13-13BB-490D9BF06F461545/DET36A_M-Manual.pdf, DET36A(/M) Si Biased Detector User Guide.
[45] S. Yeoh, M.Z. Matjafri, K.N. Mutter, A.A. Oglat, Plastic fiber evanescent sensor in measurement of turbidity, Sens. Actuator A-Phys. 285 (2019) 1–7, https://doi.org/10.1016/j.sna.2018.10.042.
[46] https://www.malvernpanalytical.com/en/assets/BRMastersizer3000EN2_tcm50-58994.pdf.
[47] T. Butt, J. Miles, P. Ganderton, P. Russell, A simple method for calibrating optical backscatter sensors in high concentrations of non-cohesive sediments, Mar. Geol. 192 (2002) 419–424, https://doi.org/10.1016/S0025-3227(02)00594-7.
[48] G.C. Kineke, R.W. Sternberg, Measurements of high concentration suspended sediments using the optical backscatterance sensor, Mar. Geol. 108 (1992) 253–258, https://doi.org/10.1016/0025-3227(92)90199-r.
[49] G. Berkovic, E. Shafir, Optical methods for distance and displacement measurements, Adv. Opt. Photon. 4 (2012) 441–471, https://doi.org/10.1364/AOP.4.000441.
[50] N.J. Clifford, K.S. Richards, R.A. Brown, S.N. Lane, Laboratory and field assessment of an infrared turbidity probe and its response to particle size and variation in suspended sediment concentration, Hydrol. Sci. J. 40 (1995) 771–791, https://doi.org/10.1080/02626669509491464.
[51] J.A.C. Bunt, P. Larcombe, C.F. Jago, Quantifying the response of optical backscatter devices and transmissometers to variations in suspended particulate matter, Cont. Shelf Res. 19 (1999) 1199–1220, https://doi.org/10.1016/S0278-4343(99)00018-7.
[52] M.N. Landers, T.W. Sturm, Hysteresis in suspended sediment to turbidity relations due to changing particle size distributions, Water Resour. Res. 49 (2013) 5487–5500, https://doi.org/10.1002/wrcr.20394.
[53] F. Druine, R. Verney, J. Deloffre, J.P. Lemoine, M. Chapalain, V. Landemaine, R. Lafite, In situ high frequency long term measurements of suspended sediment concentration in turbid estuarine system (Seine Estuary, France): Optical turbidity sensors response to suspended sediment characteristics, Mar. Geol. 400 (2018) 24–37, https://doi.org/10.1016/j.margeo.2018.03.003.
[54] J.B. Tu, D.D. Fan, Y. Zhang, G. Voulgaris, Turbulence, Sediment-Iuduced Stratification, and Mixing under Macrotidal Estuarine Conditions (Qiantang Estuary, China), J. Geophys. Res.-Oceans 124 (2019) 4058–4077, https://doi.org/10.1029/2018JC014281.
[55] J. Guillén, A. Palanques, P. Puig, X.D. De Madron, F. Nyffeler, Field calibration of optical sensors for measuring suspended sediment concentration in the western Mediterranean, Sci. Mar. 64 (2000) 427–435, https://doi.org/10.3989/scimar.2000.64n4427.
[56] C.J. Buonassissi, H.M. Dierssen, A regional comparison of particle size distributions and the power law approximation in oceanic and estuarine surface waters, J. Geophys. Res.-Oceans 115 (2010) C10028, https://doi.org/10.1029/2010JC006256.
[57] E. Kellner, J.A. Hubbart, Spatiotemporal variability of suspended sediment particle size in a mixed-land-use watershed, Sci. Total Environ. 615 (2018) 1164–1175, https://doi.org/10.1016/j.scitotenv.2017.10.040.